Sfrp1 and *Sfrp2* regulate anteroposterior axis elongation and somite segmentation during mouse embryogenesis

Wataru Satoh[1,2,3], Takafumi Gotoh[4], Yasuhiko Tsunematsu[3], Shinichi Aizawa[1,2] and Akihiko Shimono[1,*]

Regulation of Wnt signaling is essential for embryonic patterning. Sfrps are secreted Wnt antagonists that directly interact with the Wnt ligand to inhibit signaling. Here, we show that *Sfrp1* and *Sfrp2* are required for anteroposterior (AP) axis elongation and somitogenesis in the thoracic region during mouse embryogenesis. Double homozygous mutations in *Sfrp1* and *Sfrp2* lead to severe shortening of the thoracic region. By contrast, a homozygous mutation in one or the other exerts no effect on embryogenesis, indicating that *Sfrp1* and *Sfrp2* are functionally redundant. The defect of a shortened thoracic region appears to be the consequence of AP axis reduction and incomplete somite segmentation. The reduction in the AP axis is partially due to abnormalities in cell migration of pre-somitic mesoderm from the end of gastrulation. Aberrant somite segmentation is associated with altered oscillations of Notch signaling, as evidenced by abnormal *Lfng* and *Hes7* expression during somitogenesis in the thoracic region. This study suggests that Wnt regulation by Sfrp1 and Sfrp2 is required for embryonic patterning.

KEY WORDS: *Sfrp1*, *Sfrp2*, Wnt signaling, Wnt antagonists, Embryonic patterning, Somitogenesis

INTRODUCTION

Cell-cell communication is essential for embryogenesis with respect to cell fate specification, cell polarity, cell behavior and embryonic patterning. Intercellular communication is critically controlled by signaling molecules that include ligand-receptor pairs and their antagonists. Although activation of signaling via interactions between ligands and receptors exerts profound effects, the regulation of activity by secreted antagonists is indispensable for proper cell-cell communication (Niehrs, 1999; Perea-Gomez et al., 2002).

Wnt, a family of secreted glycoproteins, stimulates signals through the seven transmembrane receptors of Frizzled (Kawano and Kypta, 2003). Wnt interactions with Frizzled and the co-receptor Lrp5/Lrp6 activate the canonical Wnt/β-catenin pathway, which leads to the stabilization of β-catenin as a transcriptional regulator in the nucleus (Kawano and Kypta, 2003; Kelly et al., 2004). A proportion of Wnt molecules activate the non-canonical planar cell polarity (PCP) pathways, which results in activation of Rho GTPases, or the Wnt/Ca^{2+} pathway, which leads to intercellular Ca^{2+} release, and PKC and CamKII activation (Kühl, 2002). Nineteen Wnt genes have been identified in the human and murine genomes. Studies of loss-of function mutations in the mouse, and knockdown or overexpression in *Xenopus*, chicken and zebrafish, have revealed that Wnt proteins play diverse roles during embryogenesis in vertebrates. Wnt signaling is required for primitive streak formation (Liu et al., 1999), mesoderm cell movement (Heisenberg et al., 2000; Ulrich et al., 2003), generation of the tail organizer (Agathon et al., 2003), posterior patterning and somitogenesis (Takada et al., 1994; Aulehla et al., 2003) (see also http://www.stanford.edu/~rnusse/wntwindow.html).

[1]Vertebrate Body Plan, Center for Developmental Biology, RIKEN Kobe, Minatojima-Minami, Chuou-ku, Kobe 650-0047, Japan. [2]The Graduate School of Biological Sciences, Nara Institute of Science and Technology, 8916-5 Takayama, Ikoma, Nara, 630-0101, Japan. [3]Applied Biological Science, Faculty of Science and Technology, Tokyo University of Science, 641 Yamazaki, Noda-shi, Chiba 278-8510, Japan. [4]Kuju Agricultural Research Center, Kyushu University Graduate School of Agriculture, Naoiri-gun Kuju-cho 878-0201, Japan.

*Author for correspondence (e-mail: ashimono@cdb.riken.jp)

Wnt signaling is inhibited by several secreted antagonists: Dkk, Wise, Wif and Sfrp (Kawano and Kypta, 2003; Yamaguchi, 2001). Dickkopf (Dkk) and Wnt modulator in surface ectoderm (Wise) interact with co-receptor Lrp6, leading to the inhibition of active ligand-receptor complex formation (Semënov et al., 2001; Itasaki et al., 2003). Secreted frizzled-related protein (Sfrp) and Wnt inhibiting factor (Wif) possess a region related to the cysteine-rich domain (CRD) of Frizzled that interacts with the Wnt ligand (Hsieh et al., 1999; Kawano and Kypta, 2003). This inhibition of the ligand might regulate the degree of active Wnt in tissues (i.e. regulation of ligand activity and gradient generation). Regulation of Wnt signaling by secreted antagonists has been implicated in anterior embryonic patterning. During mouse embryogenesis, inhibition of Wnt activity by Dkk1 is necessary for anterior head specification and limb patterning (Mukhopadhyay et al., 2001). In *Xenopus*, overexpression experiments revealed that Dkk1 and FrzB (a member of the Sfrps) antagonize Wnt in the Spemann organizer, which is required for head organizer activity (Glinka et al., 1997; Leyns et al., 1997; Wang et al., 1997; Niehrs, 1999).

The Sfrp gene family consists of five members in both the human and mouse genomes (Kawano and Kypta, 2003), which are divided into Sfrp1 and FrzB subfamilies based on amino acid sequence similarity. In addition, *Crescent* and *Sizzled* are unique members found in *Xenopus* and zebrafish. *Sfrp1*, *Sfrp2* and *Sfrp5* belong to the Sfrp1 subfamily (Jones and Jomary, 2002), whose members share homology in the CRD domain. Consequently, Sfrp1, Sfrp2 and Sfrp5 suppress the canonical Wnt/β-catenin signal, decrease β-catenin levels and downregulate target gene expression, such as *Myc* expression, in cultured cells (Suzuki et al., 2004). Tlc, the zebrafish ortholog of Sfrp1 and Sfrp5, antagonizes Wnt8b in order to establish the telencephalon (Houart et al., 2002). In vitro data and *Xenopus* experiments suggest that Sfrp1 (FrzA) interacts with Wnt1, Xwnt8 and Wnt2, but not with Wnt5a (Xu et al., 1998; Dennis et al., 1999). Furthermore, Sfrp1 also interacts with Wnt7b, and is capable of attenuating the non-canonical Wnt signaling pathway, leading to inhibition of axon guidance (Rosso et al., 2005). Thus, Sfrps exhibit a wide spectrum of functions with respect to regulation of the activity of Wnt

proteins in both the canonical and non-canonical pathways. However, the functions of the Sfrps in embryogenesis have not been fully elucidated.

In this study, *Sfrp1* and *Sfrp2* double mutant mice were generated to reveal the functions of Sfrp1 subfamily members during embryogenesis. The findings demonstrate that *Sfrp1* and *Sfrp2* exhibit highly redundant functions during embryogenesis. Furthermore, the results suggest that regulation of Wnt signaling by *Sfrp1* and *Sfrp2* is required for normal AP axis elongation and somitogenesis.

MATERIALS AND METHODS
Generation of *Sfrp1* and *Sfrp2* mutant mice
A 6.5-kb *Bam*HI-*Nhe*I genomic fragment of *Sfrp1*, containing the first exon, was obtained from the C57BL/6 BAC clone (BACPAC resources) and subcloned into a plasmid to produce a *Sfrp1* knock-in (KI) vector. The KI vector contained a 5′ 1.4-kb *Bam*HI-*Sac*II fragment and a 3′ 5.3-kb *Eag*I-*Nhe*I fragment of the initially subcloned fragment (see Fig. S1 in the supplementary material). The coding sequence of the first exon was deleted and replaced with a nuclear-localized *lacZ* KI cassette (generated by Dr Maki Wakamiya, M. D. Anderson Cancer Center, The University of Texas). β-galactosidase (β-gal) staining revealed that reporter expression mimicked endogenous *Sfrp1* expression (data not shown). The *Sfrp2* targeting construct was generated from a 14-kb *Bam*HI fragment containing the entire *Sfrp2* coding sequence in the C57BL/6 BAC clone. The vector contained a 5′ 2.0-kb *Asp*718-*Eco*RI fragment and a 3′ 6.5-kb *Eco*RV-*Bam*HI fragment of the subcloned fragment (see Fig. S1 in the supplementary material). Electroporation of the vectors into embryonic stem (ES) cells and identification of homologous recombination events were performed with a strategy similar to that of Shimono and Behringer (Shimono and Behringer, 2003).

Immunostaining
For whole embryo immunostaining against neurofilament, embryos were fixed in 3.5% paraformaldehyde (PFA) in phosphate-buffered saline (PBS) at 4°C overnight. The embryos were hydrated in an ascending methanol series (25, 50, 75, 100%) in PBS containing 0.1% Tween-20 (PBT) before being re-hydrated in a descending methanol series (75, 50, 25, 0%). Following treatment with PBT containing 6% H_2O_2 and a wash in Tris-buffered saline containing 0.1% Tween-20 (TBST), embryos were treated for blocking in TBST containing 10% sheep serum. The embryos were incubated with a 2H3 monoclonal neurofilament antibody (supernatant, 1/50 dilution) at 4°C overnight. Embryos were then incubated with anti-mouse IgG antibody conjugated with HRP (1/1000 dilution). Immunoreactivity was detected with diaminobenzidine. Antibody staining against diphosphorylated ERK was conducted according to a previous report (Corson et al., 2003).

To detect non-phospho β-catenin, embryos were fixed in 8% PFA in PBS. Cryosections were subsequently generated according to a general protocol (Wakamatsu et al., 1993). Primary antibody against non-phospho β-catenin (Upstate; mouse monoclonal 8E4) was used at a 1:400 dilution, with TBST containing 5% skim milk. Immunoreactivity was detected with Alexa488-conjugated anti-mouse IgG antibody (Molecular Probes) diluted 1:200 with TBST containing 3% BSA. Images were captured on a BioRad Radiance 2100 Laser Scanning Confocal Microscope System equipped with a Zeiss Axiovert, and processed with Adobe Photoshop CS.

In situ hybridization
In situ hybridization using digoxigenin (DIG)-labeled riboprobes was performed on whole-mount embryos according to Wilkinson (Wilkinson, 1992). Some embryos were processed to generate cryosections. Double whole-mount in situ hybridizations were conducted according to Wilkinson (Wilkinson, 1992), with modifications, using two differentially labeled probes: one labeled with DIG and the other with fluorescein (FITC). After hybridization using two different probes at same time, DIG-labeled RNA probe was detected with alkaline phosphatase-conjugated anti-DIG antibody in color solution containing NBT (Nitro-Blue Tetrazolium Chloride)/BCIP (5-Bromo-4-chloro-3-indolyl phosphate, toluidine salt). Following the

primary detection procedure, the antibody was removed by washing with 0.1 M Glycine-HCl containing 0.1% Tween-20. A secondary detection procedure was then performed with an alkaline phosphatase-conjugated anti-FITC antibody in INT [2-(4-Iodophenyl)-3-(4-nitrophenyl)-5-phenyl-tetrazolium chloride]/BCIP solution.

Hoxa7 (BC036986) and *Hoxd10* (BC048690) cDNA were obtained as IMAGE clones from Invitrogen. *Axin2* (AK084644), *Fgf17* (AK077555) and *Nkd1* (AK082367) cDNA were obtained as FANTOM clones (RIKEN). A 1.5-kb fragment containing the 3′ UTR of *Hoxb2* cDNA was isolated from the E8.5 cDNA library (a gift from Dr H. Hamada, Osaka University). Images were captured with a Pixera Pro600ES digital camera, with a Zeiss Stemi2000-C stereomicroscope.

DiI cell labeling, whole-embryo and tail-bud culture
Whole-embryo culture and DiI (1,1′-dioctadecyl-3,3,3′,3′-tetra-methylindocarbocyanine perchlorate) labeling were performed according to the method of Shimono and Behringer (Shimono and Behringer, 2003). DiI was injected at the primitive streak region in the tail bud in order to label mesoderm cells. Labeled cells within the endoderm layer and the neural plate did not spread during the shorter culture period. Mesoderm cell labeling was also confirmed in cryosections of the cultured embryos. Labeled embryos, which were selected based on a lateral view of the labeling of three germ layers, were cultured for two hours. The images were captured with a Zeiss AxioCam HRc digital camera with a Leica MZFLIII fluorescence stereomicroscope. The culture was extended up to 22 hours to confirm a contribution of the labeled cells to the pre-somitic mesoderm (PSM). Embryos displaying labeled PSM cells were adopted (*n*). Tail-bud culture was performed based on the method of Correia and Conlon (Correia and Conlon, 2000).

RESULTS
Generation of *Sfrp1* and *Sfrp2* mutant mice
Sfrp1 and *Sfrp2* mutations were introduced via a deletion of the first exon encoding the first methionine and the CRD domain to generate mutant mice. For the *Sfrp1* KI mutant, the first exon was replaced with a nuclear-localized *lacZ* knock-in cassette in ES cells (see Fig. S1A,B in the supplementary material). Similarly, the first exon of *Sfrp2* was replaced with a PGKneobpAloxB cassette (Shimono and Behringer, 2003) to generate conventional knockout mice (see Fig. S1D,E in the supplementary material). Following germline transmission, mutant pups were obtained from the intercross of heterozygous mutant mice with 129 and C57BL/6 mixed backgrounds. Genotypes of the pups were determined by Southern hybridization or PCR amplification at weaning, suggesting that mice carrying the homozygous mutation in *Sfrp1* (*Sfrp1$^{-/-}$*) appeared normal during embryogenesis (see Fig. S1C, Table S1 in the supplementary material) (Bodine et al., 2004). Similarly, most of the *Sfrp2* homozygous mutant (*Sfrp2$^{-/-}$*) mice appeared normal and healthy (Fig. S1F, Table S1 in the supplementary material), although hindlimb syndactyly occurred at a lower frequency (3%; two out of 62 *Sfrp2$^{-/-}$* pups). The deleted exons encode the first methionine and the functional domain of the protein. As a result, the mutant mice were regarded as functionally null. In addition, expression of the transcript from the mutated alleles was undetectable (data not shown).

Sfrp1 and *Sfrp2* genes are functionally redundant
Functional redundancy between *Sfrp1* and *Sfrp2* has been suggested on the basis of the similarity of their expression patterns during embryogenesis. Overlapping expression of *Sfrp1* and *Sfrp2* is evident in the forebrain, midbrain and hindbrain region and in the posterior neural plate/tube at embryonic day (E) 8.5 and E9.5 (Leimeister et al., 1998). A different study reported overlapping expression in the PSM (Lee et al., 2000). Therefore, *Sfrp1$^{-/-}$;Sfrp2$^{+/-}$* mice, which appeared normal and healthy, were

intercrossed to generate *Sfrp1* and *Sfrp2* double homozygous mutant mice ($Sfrp1^{-/-};Sfrp2^{-/-}$). No $Sfrp1^{-/-};Sfrp2^{-/-}$ pups were recovered, suggesting pre-natal lethality of this mutation (see Tables S1, S2 in the supplementary material). Thus, *Sfrp1* and *Sfrp2* are functionally redundant.

$Sfrp1^{-/-};Sfrp2^{-/-}$ embryos display severe shortening of the thoracic region

$Sfrp1^{-/-};Sfrp2^{-/-}$ embryos, which died at around E16.5, exhibited edematous, craniofacial defects, limb outgrowth defects and extra digits (Fig. 1A-E; see also Table S2 in the supplementary material). The limb outgrowth defect is a typical phenotype induced by activated Wnt/β-catenin signaling, such as constitutively active β-catenin expression, Wnt overexpression and *Wnt5a* inactivation (Topol et al., 2003; Guo et al., 2004). Extra digits were frequently observed in the anterior portion of the right hindlimb (50% of embryos, *n*=16), but rarely in the left hindlimb (Fig. 1F-I), a finding that was correlated with extra stripes of *Fgf8* expression domains on the ventral surface of the hindlimb bud at E10.5 (Fig. 1J,K). Ectopic *Fgf8* expression has been associated with an upregulation of Wnt/β-catenin signaling in the apical ectodermal ridge during limb morphogenesis (Mukhopaghyay at al., 2001; Barrow et al., 2003; Soshnikova et al., 2003). *Sfrp1* is expressed in the ventral body wall, including the proximal region of the hindlimb bud, and *Sfrp2* is expressed in the limb mesenchyme at E10.5 (Leimeister et al., 1998).

Patterning in the forebrain, midbrain and hindbrain of $Sfrp1^{-/-};Sfrp2^{-/-}$ embryos appeared normal up to E9.5-E10.5. Although *Sfrp1* and *Sfrp2* are highly expressed in the hindbrain (Leimeister et al., 1998), rhombomere patterning was normal in $Sfrp1^{-/-};Sfrp2^{-/-}$ embryos, as evidenced by staining for *Krox20*

transcripts in rhombomeres 3 and 5, and immunoreactivity staining with the 2H3 anti-neurofilament monoclonal antibody (data not shown).

Gross morphology suggested that the entire AP body axis was shortened in $Sfrp1^{-/-};Sfrp2^{-/-}$ embryos at E14.5-E16.5. Moreover, cartilage staining revealed that the thoracic region was severely shortened, and that the number of thoracic vertebrae was reduced from thirteen to five (Fig. 1B-E). This observation suggested that AP axis formation, especially in the thoracic region, might be affected in $Sfrp1^{-/-};Sfrp2^{-/-}$ embryos in a manner that correlates axis elongation with somite segmentation. To elucidate the body axis at the marker level, expression of the following Hox genes was examined at E9.25-E10.5: *Hoxb2*, whose anterior expression boundary is located at rhombomere 3 (Rossel and Capecchi, 1999); *Hoxa7*, which has an anterior boundary in the mesoderm at the thirteenth somite (Li and Shiota, 1999); and *Hoxd10*, which is expressed up to the twenty-seventh somite (Hérault et al., 1998). *Hoxb2* was expressed in the posterior region from rhombomere 3 in $Sfrp1^{-/-};Sfrp2^{-/-}$ embryos, as well as in the control (wild type, $Sfrp1^{-/-};Sfrp2^{+/+}$ and $Sfrp1^{-/-};Sfrp2^{+/-}$) embryos (Fig. 2A,B). The anterior boundary of *Hoxa7* expression in the mesoderm was located around the thirteenth somite in the $Sfrp1^{-/-};Sfrp2^{-/-}$ embryos, a pattern similar to that of the control embryos at E9.25 (Fig. 2C,D). However, using myogenin expression as the landmark in the double whole-mount in situ hybridizations (Fig. 2E-H) (Edmondson and Olson, 1989), the expression boundary of *Hoxd10* was shifted to the twenty-first somite in $Sfrp1^{-/-};Sfrp2^{-/-}$ embryos at E10.5 (Fig. 2E,F). These observations suggest that somites 11-23, which give rise to vertebrae in the thoracic region, are fused, and/or reduced in number, during somite segmentation (Fig. 2I).
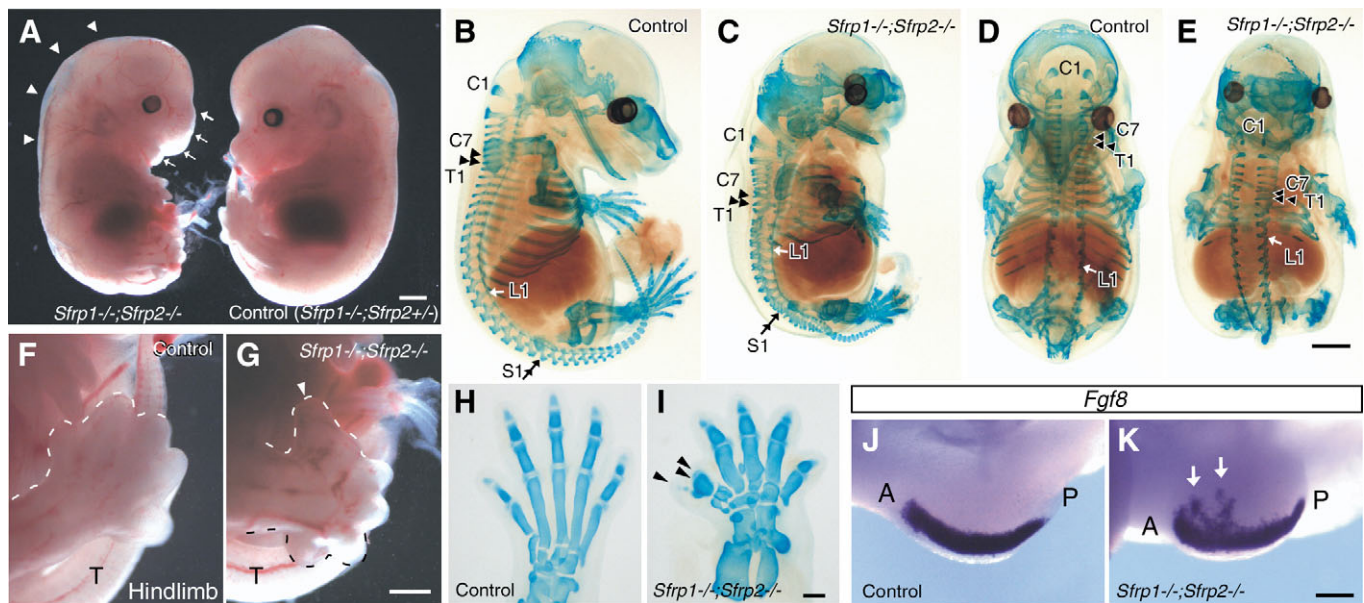

Fig. 1. $Sfrp1^{-/-};Sfrp2^{-/-}$ embryos display shortening of the thoracic region and limb morphogenesis abnormality. (A) Gross morphology of $Sfrp1^{-/-};Sfrp2^{-/-}$ mutant (left) and control (right) embryos at E14.5. Arrows indicate the craniofacial abnormality; arrowheads indicate edematous defects. Scale bar: 1 mm. **(B-E)** Cartilage staining in control (B,D) and $Sfrp1^{-/-};Sfrp2^{-/-}$ (C,E) embryos at E15.5. The number of thoracic vertebrae was reduced in $Sfrp1^{-/-};Sfrp2^{-/-}$ embryos. Although vertebrae numbers were normal, the sides of vertebrae were reduced in the lumbar and sacral regions. Arrowhead, C7 vertebra; double arrowhead, T1 vertebra; single arrow, L1 vertebra; double arrow, S1 vertebrae; C1, atlas. Scale bar: 1 mm. **(F-I)** Extra digits (arrowhead) on the hindlimb of $Sfrp1^{-/-};Sfrp2^{-/-}$ embryos (G) at E14.5, and the skeletal pattern of the hindlimb in control (H) and $Sfrp1^{-/-};Sfrp2^{-/-}$ (I) embryos at E15.5. T, tail. Scale bars: 500 μm in F,G; 200 μm in H,I. **(J,K)** *Fgf8* expression in the limb bud of control (J) and $Sfrp1^{-/-};Sfrp2^{-/-}$ (K) embryos at E10.5. Arrows indicate the extra stripes of *Fgf8* expression in the ventral surface of the hindlimb bud. A, anterior; P, posterior. Scale bar: 400 μm.
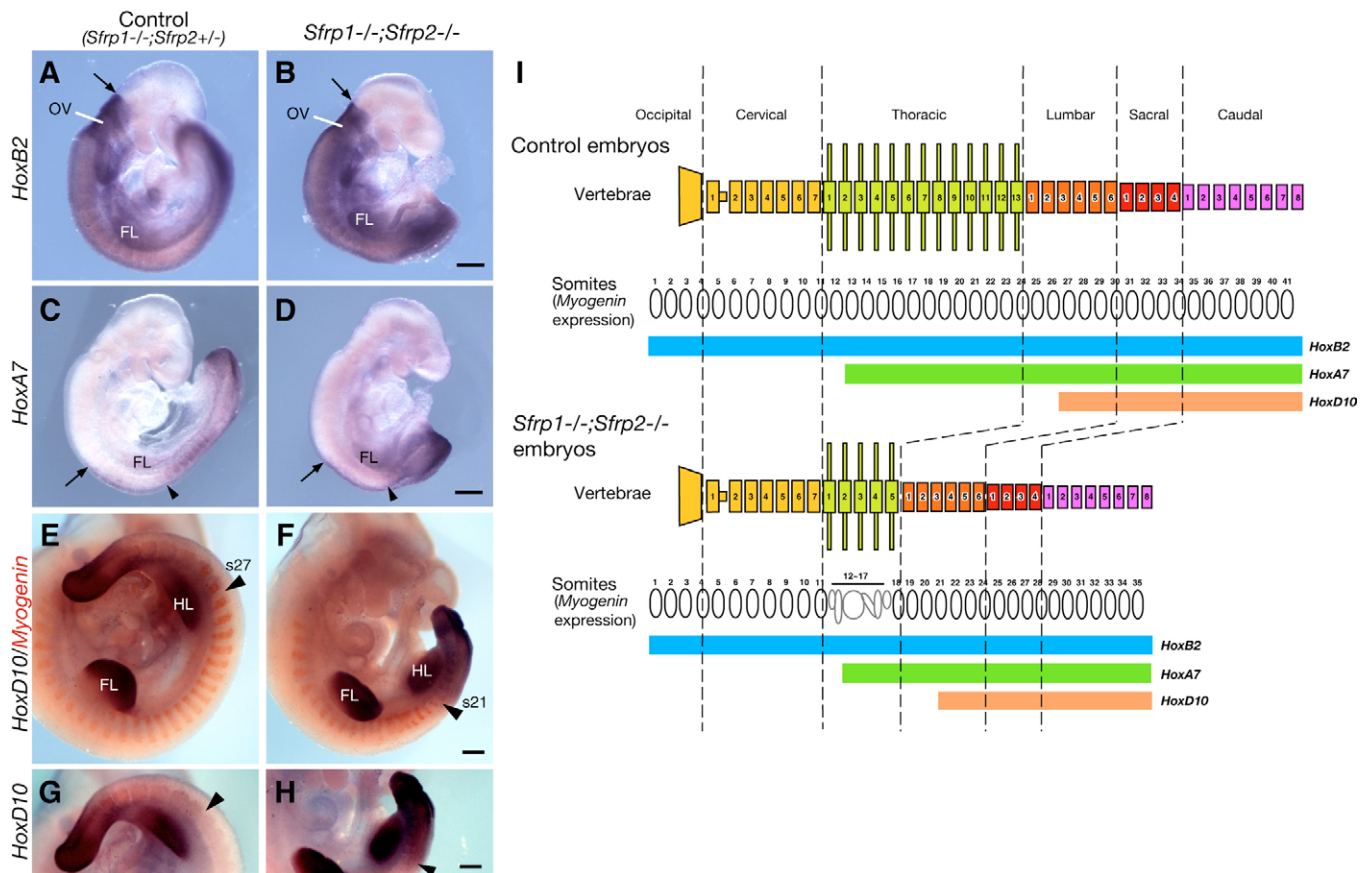
Fig. 2. *Hox* **gene expression in** *Sfrp1$^{-/-}$;Sfrp2$^{-/-}$* **embryos.** (**A**,**B**) *Hoxb2* expression in control (A) and *Sfrp1$^{-/-}$;Sfrp2$^{-/-}$* (B) embryos at E9.25. An arrow indicates the anterior boundary of *Hoxb2* expression at rhombomere 3. ov, otic vesicle. (**C**,**D**) *Hoxa7* expression in control (C) and *Sfrp1$^{-/-}$;Sfrp2$^{-/-}$* (D) embryos at E9.25. An arrow and an arrowhead indicate the anterior boundary of *Hoxa7* expression in the spinal cord and somite, respectively. (**E-H**) *Hoxd10* and myogenin gene expression in control (E,G) and *Sfrp1$^{-/-}$;Sfrp2$^{-/-}$* (F,H) embryos at E10.5. Myogenin expression was visualized by INT/BCIP in double in situ hybridization (red). An arrowhead depicts the anterior boundary of *Hoxd10* in the somite. (**I**) Summary of the skeletal pattern and *Hoxb2*, *Hoxa7* and *Hoxd10* expression in control and *Sfrp1$^{-/-}$;Sfrp2$^{-/-}$* embryos. Correlation between vertebrae and somite number (12-17) was estimated from myogenin expression in *Sfrp1$^{-/-}$;Sfrp2$^{-/-}$* embryos (E,F). FL, forelimb; HL, hindlimb. Scale bars: 250 μm.

Somitogenesis in *Sfrp1$^{-/-}$;Sfrp2$^{-/-}$* embryos

Histological analysis disclosed randomized, incomplete segmentation of somites in *Sfrp1$^{-/-}$;Sfrp2$^{-/-}$* embryos at E9.5 (Fig. 3A-D). A segmentation defect in the middle of the trunk at E10.5 was also revealed by immunostaining with an anti-neurofilament antibody (Fig. 3E,F) (Dodd et al., 1988). Histological analysis showed randomized segmentation after the eleventh somite in the region between the forelimb and the hindlimb (Fig. 3C,D). This finding was confirmed by marker analysis of *Mox1* (Fig. 4A-D), which is expressed in somites from the onset of segmentation and is gradually restricted to the posterior half-somite of sclerotome lineage (Candia et al., 1992), and of *Pax3* (Fig. 4E-H), a marker for the dermatome lineage (Goulding et al., 1991). Regular, albeit smaller, somites were generated in a posterior region near the hindlimb, as well as around the forelimb level, suggesting restoration of somite segmentation around the hindlimb level (Figs 3, 4). The somites maintained AP identity within the region between the forelimb and the hindlimb, and the abnormal somites expressed *Uncx4.1* and *Pax1*, markers for the sclerotome lineage (Mansouri et al., 1997; Neubuser et al., 1995) (Fig. 4I-K; data not shown). Although myotome differentiation was delayed in the embryos, as indicated by myogenin expression at E9.5 (Edmondson and Olson, 1989) (Fig. 4L-N), these observations reveal that cell differentiation occurs in

somites with impaired segmentation. Significantly, myogenin expression at E10.5 clearly demonstrated a reduced number of somites between the forelimb and hindlimb in *Sfrp1$^{-/-}$;Sfrp2$^{-/-}$* embryos (17 somites in *Sfrp1$^{-/-}$;Sfrp2$^{+/+}$* or *Sfrp1$^{-/-}$;Sfrp2$^{+/-}$* embryos, *n*=3; 13 somites in *Sfrp1$^{-/-}$;Sfrp2$^{-/-}$* embryos, *n*=3; Fig. 4R-T). Moreover, the pre-somitic mesoderm (PSM) region was dramatically reduced in the *Sfrp1$^{-/-}$;Sfrp2$^{-/-}$* embryos, as evidenced by the expression pattern of the delta-like 1 gene (*Dll1*) (Bettenhausen et al., 1995) at E9.5 (Fig. 4O-Q). This observation, in addition to the small somite around the forelimb level, is suggestive of a defect in posterior embryonic patterning at an early stage. The defect of posterior patterning was apparent as a reduction in the posterior axis at E8.25, and appeared prior to small somite generation and irregular and incomplete somite segmentation.

Sfrp1 and *Sfrp2* are required for AP axis elongation in the thoracic region

Sfrp1$^{-/-}$;Sfrp2$^{-/-}$ embryos were indistinguishable from wild-type and control embryos at the late head-fold stage. However, the *Sfrp1$^{-/-}$;Sfrp2$^{-/-}$* embryos, which had begun to generate somites, were distinct from control embryos in the posterior region in the increased thickness of the mesoderm layer (a bar in the tail region, Fig. 5A-C). The expression patterns of brachyury (*T*), *Tbx6* and *Dll1*
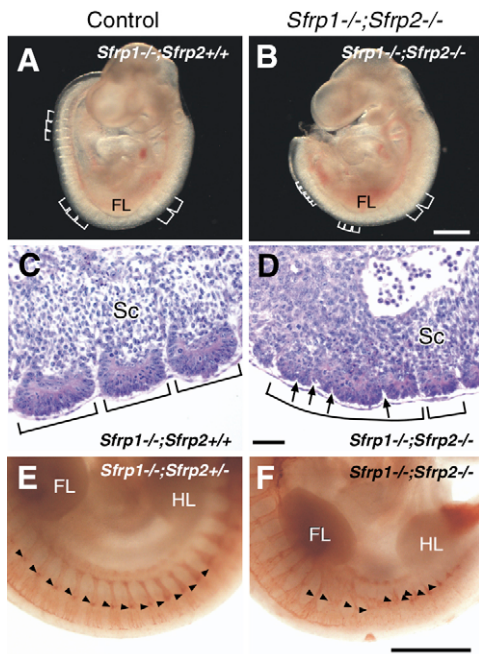
Fig. 3. Somite segmentation abnormality in *Sfrp1⁻/⁻;Sfrp2⁻/⁻* embryos. (**A,B**) Gross morphology of control (*Sfrp1⁻/⁻;Sfrp2⁺/⁺*; A) and *Sfrp1⁻/⁻;Sfrp2⁻/⁻* (B) embryos at E9.5. Somite size is indicated by a bracket. Inactivation of *Sfrp1* and *Sfrp2* resulted in reduced length of the posterior region. Scale bar: 500 μm. (**C,D**) Somite segmentation was aberrant in *Sfrp1⁻/⁻;Sfrp2⁻/⁻* embryos. Somite segmentation was examined in para-sagittal sections, which were stained with Hematoxylin and Eosin, of control (C) and *Sfrp1⁻/⁻;Sfrp2⁻/⁻* (D) embryos at E9.5. Regular and similarly sized somites (bracket) were observed in control embryos, whereas incomplete segmentation (arrows in a bracket) was apparent in the region between the forelimb and hindlimb of *Sfrp1⁻/⁻;Sfrp2⁻/⁻* embryos. Scale bar: 50 μm. (**E,F**) Immunostaining with 2H3 monoclonal anti-neurofilament antibody (arrowheads) of control (E) and *Sfrp1⁻/⁻;Sfrp2⁻/⁻* (F) embryos at E10.5. Scale bar: 500 μm. FL, forelimb; HL, hindlimb; Sc, sclerotome.

were examined in order to gain insight into the defect in posterior axis extension. *T* expression in *Sfrp1⁻/⁻;Sfrp2⁻/⁻* embryos suggested that the primitive streak and the axial mesoderm (node and notochord) were generated normally in the early somite stage (~three somites) (Fig. 5A-C) (Wilkinson et al., 1990). *Tbx6* and *Dll1* were expressed in the PSM region (between the arrow and arrowhead in Fig. 5D,E,G,H; data not shown) and in the paraxial mesoderm of the primitive streak region (between the bar and arrow in Fig. 5D,E,G,H; data not shown) in wild-type and control embryos at E8.5 (Bettenhausen et al., 1995; Chapman et al., 1996). In the *Sfrp1⁻/⁻;Sfrp2⁻/⁻* embryos, *Tbx6* and *Dll1* expression were observed with high intensity in the paraxial mesoderm on both sides of the primitive streak (between the bar and arrow in Fig. 5F,I; data not shown); moreover, anterior extension of the expression domain was greatly reduced (between the arrow and arrowhead in Fig. 5F,I; data not shown). Sections of embryos at somite stages 6/7 and 11 revealed that unusual *Dll1* staining was predominantly due to an increased number of paraxial mesoderm cells in the posterior embryonic portion (Fig. 5K,L,N,O; data not shown).

In order to identify the abnormality in posterior axis extension around E8.5, cell proliferation ratio was examined in *Sfrp1⁻/⁻;Sfrp2⁻/⁻* embryos. The cell proliferation rate, indicated by anti-phospho-Histone H3 antibody staining (a mitotic marker) (Chadee et al.,

1995), was not elevated in the posterior region of *Sfrp1⁻/⁻;Sfrp2⁻/⁻* embryos in comparison with control embryos (7.36±1.30% of anti-phospho-Histone H3-positive cells in *Sfrp1⁻/⁻;Sfrp2⁺/⁺* embryos; 6.48±1.63% in *Sfrp1⁻/⁻;Sfrp2⁻/⁻* embryos; *n*=3) at the 6 somite stage (data not shown). By contrast, the rate appeared to be reduced in *Sfrp1⁻/⁻;Sfrp2⁻/⁻* embryos at the 11 somite stage (7.83±0.73% of anti-phospho-Histone H3-positive cells in *Sfrp1⁻/⁻;Sfrp2⁺/⁺* embryos; 3.76±0.88% in *Sfrp1⁻/⁻;Sfrp2⁻/⁻* embryos; *n*=3; data not shown). Thus, a reduction in cell proliferation may contribute to a diminished posterior axis at a later stage. However, a reduction of the posterior axis in conjunction with the increased thickness in the mesoderm cell layer is evident in *Sfrp1⁻/⁻;Sfrp2⁻/⁻* embryos at the end of the head-fold stage, when cell proliferation rate is unaffected. Therefore, accumulation of *Dll1*-expressing cells appears to be a consequence of cell migration defects in mesoderm cells along the AP axis.

Cell migration was directly evaluated via cell labeling with the lipophilic dye DiI. DiI was injected into the mesoderm cell population around the primitive streak region of control and *Sfrp1⁻/⁻;Sfrp2⁻/⁻* embryos. The DiI-labeled mesoderm cells migrated into the lateral region in the control embryos (Fig. 5P,Q; *n*=14). By contrast, migration of DiI-labeled mesoderm cells was greatly reduced in *Sfrp1⁻/⁻;Sfrp2⁻/⁻* embryos (Fig. 5R,S; *n*=5). Thus, *Sfrp1* and *Sfrp2* mediate posterior axis extension via regulation of cell migration in the paraxial mesoderm.

Wnt3a is expressed in the tail bud of developing embryos (Yoshikawa et al., 1997). Because Sfrp1 and Sfrp2 possess inhibitory activity against the Wnt pathway, activation of Wnt signaling was examined in *Sfrp1⁻/⁻;Sfrp2⁻/⁻* embryos at E8.5. Activation of the Wnt/β-catenin pathway was evaluated by antibody staining against stabilized non-phospho β-catenin. A higher staining intensity in the cellular membrane and nucleus was observed in the hindgut and in the mesoderm beneath the primitive streak in control embryos (Fig. 6A,B,G-I). In *Sfrp1⁻/⁻;Sfrp2⁻/⁻* embryos, a similar staining intensity was ectopically detected in the tail bud region in the mesoderm and neural ectoderm, as well as in the hindgut endoderm and the mesoderm beneath the primitive streak (*n*=2; Fig. 6D-E,J-O). Thus, inactivation of *Sfrp1* and *Sfrp2* leads to activation of the Wnt pathway in the embryos.

Sfrp1 and *Sfrp2* affect Notch oscillatory cycles in the PSM

Wnt and Fgf8 gradients play a role in the establishment of somite segmentation boundaries (Aulehla et al., 2003). A steeper gradient in a shorter PSM region could lead to the generation of small somites. However, the shorter PSM is insufficient to account for the randomized and incomplete segmentation in *Sfrp1⁻/⁻;Sfrp2⁻/⁻* embryos. Coordinated somite segmentation is regulated by the cyclic expression of Notch related genes, such as *Lfng* and *Hes7*, in the PSM (Saga and Takeda, 2001; Bessho et al., 2001). Because *Wnt3a* is required for oscillating Notch signaling activity in the PSM (Aulehla et al., 2003), the expression of *Wnt3a* in *Sfrp1⁻/⁻;Sfrp2⁻/⁻* embryos was examined during incomplete somite segmentation and following the restoration of regular somite segmentation. The level of *Wnt3a* expression was normal in the tail bud region of *Sfrp1⁻/⁻;Sfrp2⁻/⁻* embryos displaying defective somite segmentation at E8.5 (see Fig. S2A-C in the supplementary material). In addition, *Fgf8* was normally expressed in the tail bud of these embryos (see Fig. S2J-L′ in the supplementary material). Activation of Fgf signaling, visualized with an anti-diphospho-ERK antibody (Corson et al., 2003), was observed in posterior portion of the control embryos, and showed reduced activation in anterior region of the PSM (see Fig. S2M,N in the supplementary material). Similar
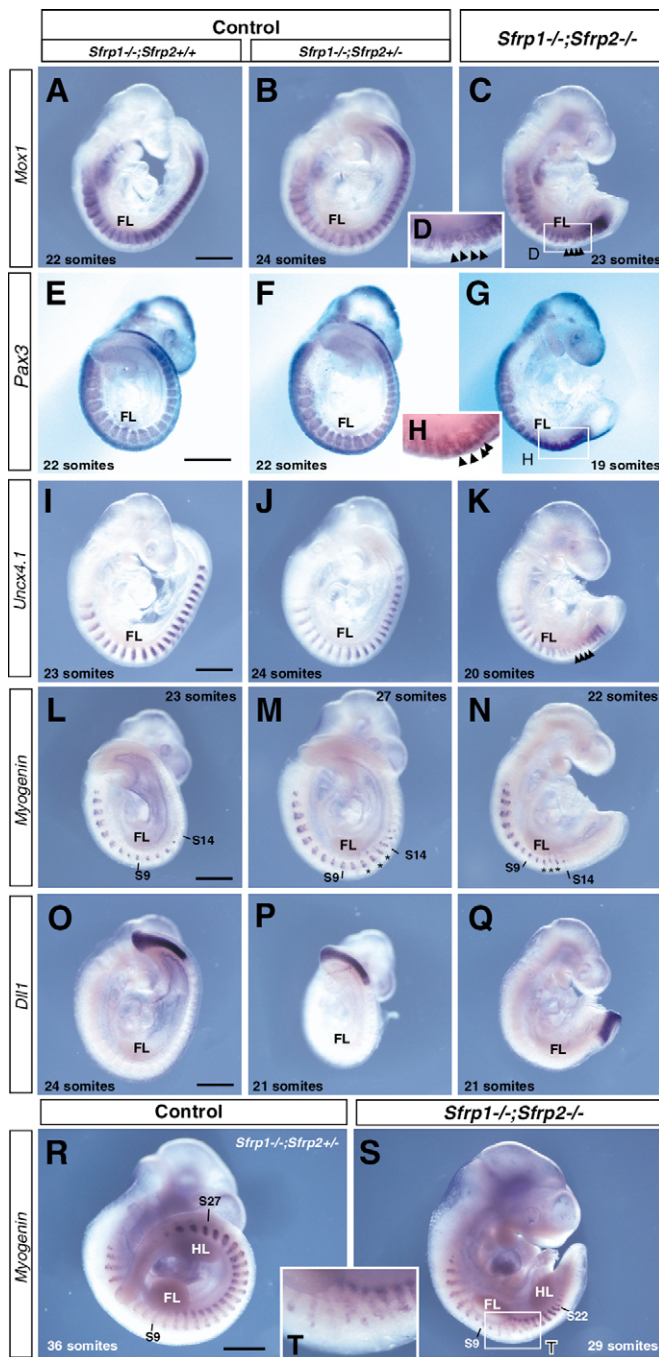
Fig. 4. Segmentation and cell differentiation in somites of Sfrp1⁻/⁻;Sfrp2⁻/⁻ embryos. (A-N) Somite segmentation was aberrant in the region between the forelimb and hindlimb in Sfrp1⁻/⁻;Sfrp2⁻/⁻ embryos. However, cell differentiation in the somite did occur in that region. (A-D) Expression of *Mox1* in control (A,B) and Sfrp1⁻/⁻;Sfrp2⁻/⁻ (C) embryos at E9.5. D shows a higher magnification of the region indicated in C. Arrowheads indicate irregular segmentation of the somite. *Pax3* (E-H), *Uncx4.1* (I-K) and myogenin (L-N) expression in control (E,F,I,J,L,M) and Sfrp1⁻/⁻;Sfrp2⁻/⁻ (G,K,N) embryos at E9.5. H shows the region indicated in G at higher magnification. Arrowheads indicate irregular segmentation of the somite. Asterisks indicate somite positions in the Sfrp1⁻/⁻;Sfrp2⁻/⁻ embryo (N) corresponding to those of the control embryo (M). (O-Q) *Dll1* expression in control (O,P) and Sfrp1⁻/⁻;Sfrp2⁻/⁻ (Q) embryos. Note that the PSM region was severely affected in the double homozygous mutant embryos. (R-T) Myogenin expression in control (R) and Sfrp1⁻/⁻;Sfrp2⁻/⁻ (S) embryos. The number of somites decreased in the region between the forelimb and hindlimb in the Sfrp1⁻/⁻;Sfrp2⁻/⁻ embryo. T displays higher magnification of the region indicated in S. FL, forelimb; HL, hindlimb. Scale bar: 500 μm.

This observation suggests the possibility that aberrant somitogenesis in Sfrp1⁻/⁻;Sfrp2⁻/⁻ embryos occurs during the portion of the segmentation process related to *Wnt3a* expression (Aulehla et al., 2003). Therefore, expression of the Notch-related oscillator genes lunatic fringe (*Lfng*) and *Hes7* was examined in Sfrp1⁻/⁻;Sfrp2⁻/⁻ embryos at somite stages 10 to 13. Dynamic expression of *Lfng*, which is regulated by Notch signaling, is required for the somite segmentation process (Forsberg et al., 1998; Evrard et al., 1998; Cole et al., 2002; Morales et al., 2002),which is altered in *Wnt3a* mutants (Aulehla et al., 2003). Oscillating expression of *Lfng* was visualized via comparison between the half tail regions with and without culture incubation; in addition, the expression pattern was precisely compared between the explants according to Forsberg et al. (Forsberg et al., 1998) (Fig. 7G). All pairs of explants derived from control embryos at E8.5 exhibited the oscillating expression pattern (*n*=18; Fig. 7A,D,G). By contrast, the oscillations were perturbed in all pairs of Sfrp1⁻/⁻;Sfrp2⁻/⁻ tail explants (*n*=7, Fig. 7B,C,E-G). An extra stripe was observed in the anterior-most region of the PSM, suggesting delayed somite segmentation (indicated by a dagger in Fig. 7C,F; two out of seven pairs of explants). Interestingly, cyclic expression of *Lfng* in the Sfrp1⁻/⁻;Sfrp2⁻/⁻ explants at E9.5 was indistinguishable from that of control explants (Fig. 7H,I; *n*=11 for control, *n*=3 for Sfrp1⁻/⁻;Sfrp2⁻/⁻ explants). Consequently, the abnormal expression pattern of the oscillator gene appears to be related to the defect in somite segmentation.

Hes7 expression is controlled by Notch signaling, and Hes7 protein represses *Lfng* expression (Bessho et al., 2001; Bessho et al., 2003). Although normal oscillating cycles of *Hes7* were consistently observed in control explants (Fig. 7J,M; *n*=6), cyclic expression was affected in the Sfrp1⁻/⁻;Sfrp2⁻/⁻ embryos (three out of five pairs of explants, Fig. 7L-O). In a manner similar to that of *Lfng* expression, a strong extra stripe frequently occurred in the anterior-most region of the PSM (indicated by a dagger in Fig. 7L,N; two out of five pairs of explants). Therefore, *Sfrp1* and *Sfrp2* affect Notch oscillator cycles.

Axin2 and *Nkd1*, negative regulators of the Wnt pathway, have been shown to exhibit an oscillatory expression pattern in the PSM (Aulehla et al., 2003; Ishikawa et al., 2004). On the one hand, Dynamic expression of *Axin2*, a Wnt-driven oscillator (Aulehla et

staining patterns were observed in the Sfrp1⁻/⁻;Sfrp2⁻/⁻ embryos (Fig. S2O in the supplementary material). However, *Wnt3a* expression decreased in the tail bud at E9.5, when somite segmentation was restored (see Fig. S3J-L in the supplementary material). In addition, *Fgf8* expression was diminished in the tail bud, which was consistent with the findings of a previous report (Aulehla et al., 2003) (Fig. S3G-I in the supplementary material). By contrast, other marker genes of the tail bud region were normally expressed in Sfrp1⁻/⁻;Sfrp2⁻/⁻ embryos (Maruoka et al., 1998; Yamguchi et al., 1999a) (Fig. S3A-F,M-O in the supplementary material). Hence, the defect is correlated with expression levels of *Wnt3a*. The reduction of *Wnt3a* expression in the tail bud may reduce the signaling activity elevated by Sfrp1 and Sfrp2 inactivation to levels that have no effect on somite segmentation.

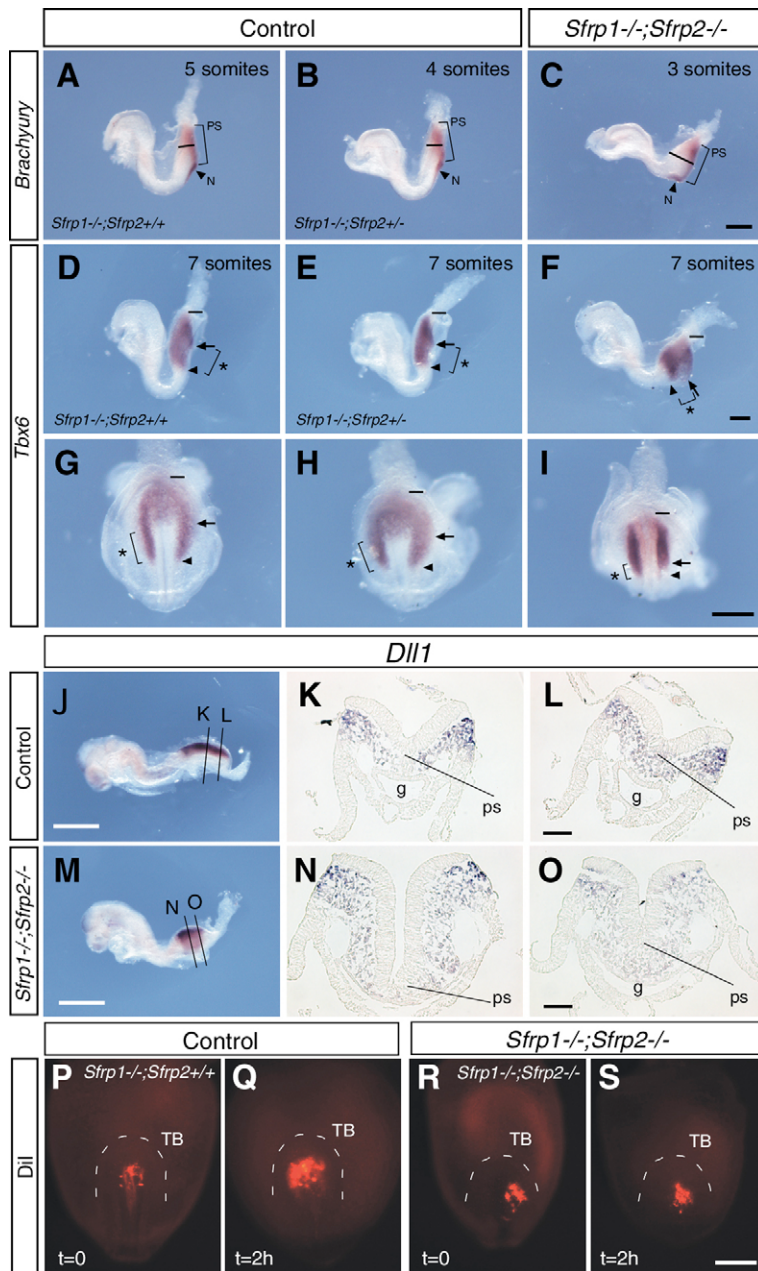**Fig. 5. Defect in posterior axis extension in *Sfrp1$^{-/-}$;Sfrp2$^{-/-}$* embryos at E8.5.** (**A-C**) Brachyury (*T*) expression in control (A,B) and *Sfrp1$^{-/-}$;Sfrp2$^{-/-}$* (C) embryos. PS, primitive streak; N, node. Defective posterior axis extension initially appeared as an increased thickness of the mesoderm layer (bar) in the posterior region of the *Sfrp1$^{-/-}$;Sfrp2$^{-/-}$* embryos when somite formation began. Scale bar: 250 μm. (**D-I**) *Tbx6* expression in control (D,E,G,H) and *Sfrp1$^{-/-}$;Sfrp2$^{-/-}$* (F,I) embryos. D-F, lateral view; G-I, posterior view. An unusually high intensity of staining was detected on both sides of the primitive streak of *Sfrp1$^{-/-}$;Sfrp2$^{-/-}$* embryos. Furthermore, the PSM region (asterisk) was markedly reduced in these embryos. Scale bars: 250 μm in D-I. (**J-O**) *Dll1* expression in control (J,K,L) and *Sfrp1$^{-/-}$;Sfrp2$^{-/-}$* (M,N,O) embryos at the 11 somite stage. K,L,N and O show cross sections of the tail bud region indicated in J and M. Cross sections were generated following in situ hybridization. Scale bars: 500 μm in J,M; 50 μm in K-L,N-O. (**P-S**) DiI cell-labeling assay of mesoderm cells in control (P,Q) and *Sfrp1$^{-/-}$;Sfrp2$^{-/-}$* (R,S) embryos at several somite stages. DiI was injected into mesoderm cells around the primitive streak (*t*=0; P,R), followed by a 2-hour culture of the embryos (*t*=2h; Q,S). TB, tail bud. Scale bar: 250 μm.

al., 2003), was observed in *Sfrp1$^{-/-}$;Sfrp2$^{-/-}$* embryo explants (*n*=5), as well as in controls (*n*=19). On the other hand, the majority of control explants (89%; total *n*=9) exhibited changes in expression levels of *Nkd1*, an oscillator gene activated downstream of Wnt signaling (Yan et al., 2001) (Fig. 7S). By contrast, most of the explants (75%; total *n*=8) derived from *Sfrp1$^{-/-}$;Sfrp2$^{-/-}$* embryos retained higher expression levels of *Nkd1* (Fig. 7T,U). This observation indicates that the downstream target of Wnt signaling is activated in the absence of *Sfrp1* and *Sfrp2*. In concert, the results derived from the explant cultures suggest that inhibition of Wnt signaling by Sfrp1 and Sfrp2 is an essential component of the somite segmentation process.

DISCUSSION
In the present paper, we provide evidence indicating that *Sfrp1* and *Sfrp2* are functionally redundant. Additionally, the results demonstrate the requirement of *Sfrp1* and *Sfrp2* with respect to

embryonic AP patterning and somitogenesis. Reduction of the AP axis was associated with mesoderm cell migration, and aberrant somite segmentation was correlated with perturbed Notch oscillator cycles.

Sfrp1 and *Sfrp2* possess redundant functions during embryonic development
It has been reported that Sfrp1 and Sfrp2 exert opposing effects on β-catenin stability in MCF-7 breast cancer cells: Sfrp1 decreased β-catenin stability, whereas Sfrp2 increased β-catenin cellular concentration (Melkonyan et al., 1997). Moreover, Sfrp2 acts as an antagonist of Sfrp1 with respect to Wnt inhibition (Yoshino et al., 2001). The generation of mice that are null for both *Sfrp1* and *Sfrp2* clearly reveals that these two proteins compensate for one another during embryonic development. Overlapping expression of the genes is observed from the early somite stage to the organogenesis period. However, the expression pattern is not completely coincident
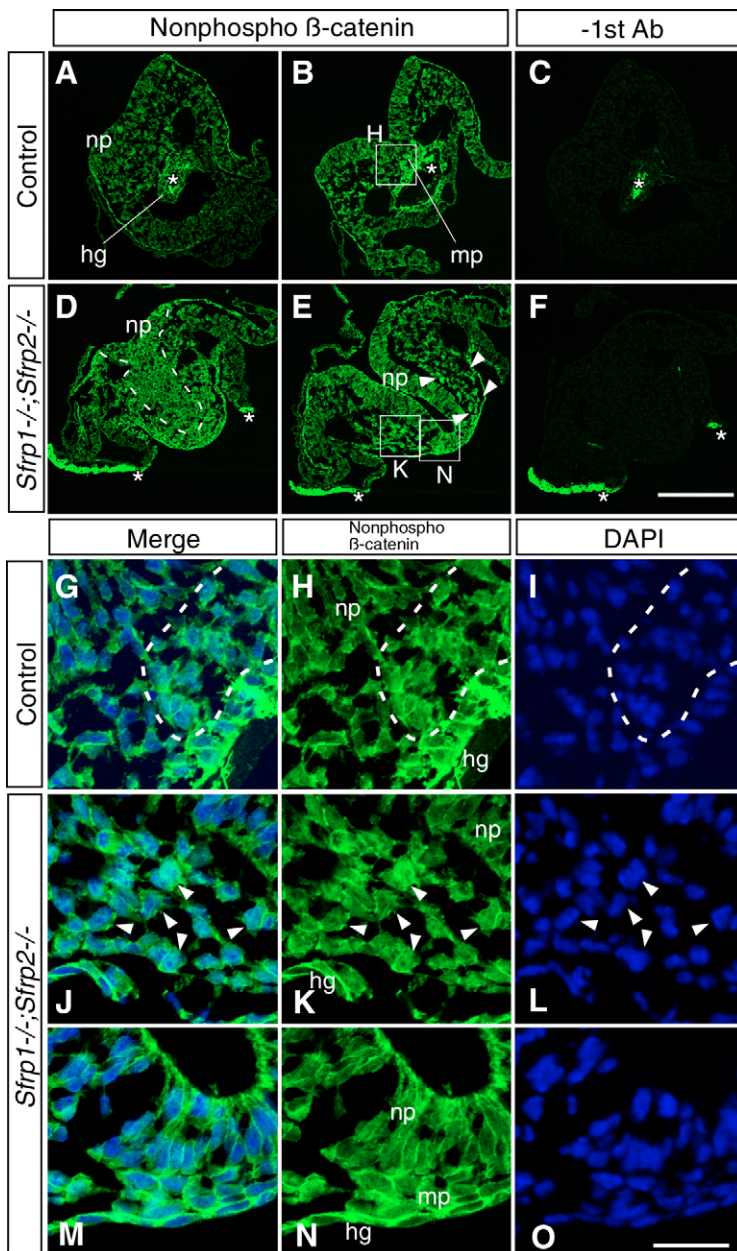
Fig. 6. Activation of the Wnt/β-catenin pathway in the tail bud of *Sfrp1⁻/⁻; Sfrp2⁻/⁻* embryos at E8.5. (**A-F**) Cross sections of the posterior region in control (A,B) and *Sfrp1⁻/⁻;Sfrp2⁻/⁻* (D,E) embryos stained with anti non-phospho β-catenin antibody. (C,F) Control staining was performed without the first antibody. hg, hindgut; mp, mesoderm cells beneath the primitive streak; np, neural plate; asterisk, non-specific staining. Higher staining intensity was observed in the hindgut and in the axial mesoderm of control embryos. A similar intensity in staining was observed in the tail bud region of *Sfrp1⁻/⁻; Sfrp2⁻/⁻* embryos, including the mesoderm, neural ectoderm and laterally located paraxial mesoderm (inside of arrowheads and in the box labelled K; E), in addition to the hindgut endoderm and mesoderm beneath the primitive streak. Scale bar: 200 μm. (**G-O**) Higher magnification of the regions (labeled H,K,N) indicated in B and E. The mesoderm beneath the primitive streak is outlined by the broken line in H. (I,L,O) Nuclei were stained with DAPI (4,6-diamino-2-phenylindole; blue). G,J and M show merged images of H and I, K and L, and N and O, respectively. Arrowheads in J (merged image) indicate the positions of cells corresponding to those in original images (K and L). Scale bar: 33 μm.

at later stages (Leimeister et al., 1998). The fact that Sfrps are secreted antagonists, rather than the differences between expression sites of the genes, could account for the functional redundancy of *Sfrp1* and *Sfrp2*.

Inhibition of Wnt signaling is required for activity of the head organizer (Niehrs, 1999). *Sfrp1* is expressed in the anterior visceral endoderm (AVE) and the anterior mesendoderm (AME), essential tissues for head formation in the mouse (Shawlot et al., 1999), whereas wider expression of *Sfrp2* is detected in the embryonic ectoderm at the primitive streak stage (Mukhopadhyay et al., 2003). *Sfrp1* cDNA was isolated in a screen of differentially expressed genes in wild-type and *Lim1* (also referred as to *Lhx1*) mutant AVE/AME at the late streak stage (Shimono and Behringer, 1999; Shimono and Behringer, 2000). *Lim1* is necessary for head organizer activity (Shawlot and Behringer, 1995; Shawlot et al., 1999). In addition, *Sfrp1* expression is reduced in the AVE and AME of *Lim1* homozygous mutant embryos (A.S., unpublished). However, no

defect was evident in anterior patterning in the *Sfrp1⁻/⁻;Sfrp2⁻/⁻* embryos. *Sfrp5* and *Dkk1* are expressed in the AVE, which may compensate for the loss of *Sfrp1* and *Sfrp2* function in anterior patterning (Mukhopadhyay et al., 2001; Finley et al., 2003).

Sfrps and Wnts signaling

The results of this study provide genetic evidence for the in vivo function of *Sfrp* genes in embryonic development. The limb defect is consistent with the phenotype induced by Wnt/β-catenin signal activation (Mukhopaghyay at al., 2001; Barrow et al., 2003; Soshnikova et al., 2003). The defect in posterior axis elongation in *Sfrp1⁻/⁻;Sfrp2⁻/⁻* embryos at E8.25 appeared to be associated with an abnormality in migration of the paraxial mesoderm cells. In addition, we observed higher activation of the Wnt/β-catenin pathway in the posterior region of *Sfrp1⁻/⁻;Sfrp2⁻/⁻* embryos. Mesoderm migration is known to be dependent on the function of *T*, a downstream target of the Wnt/β-catenin pathway (Wilson et al., 1993; Yamaguchi et al.,
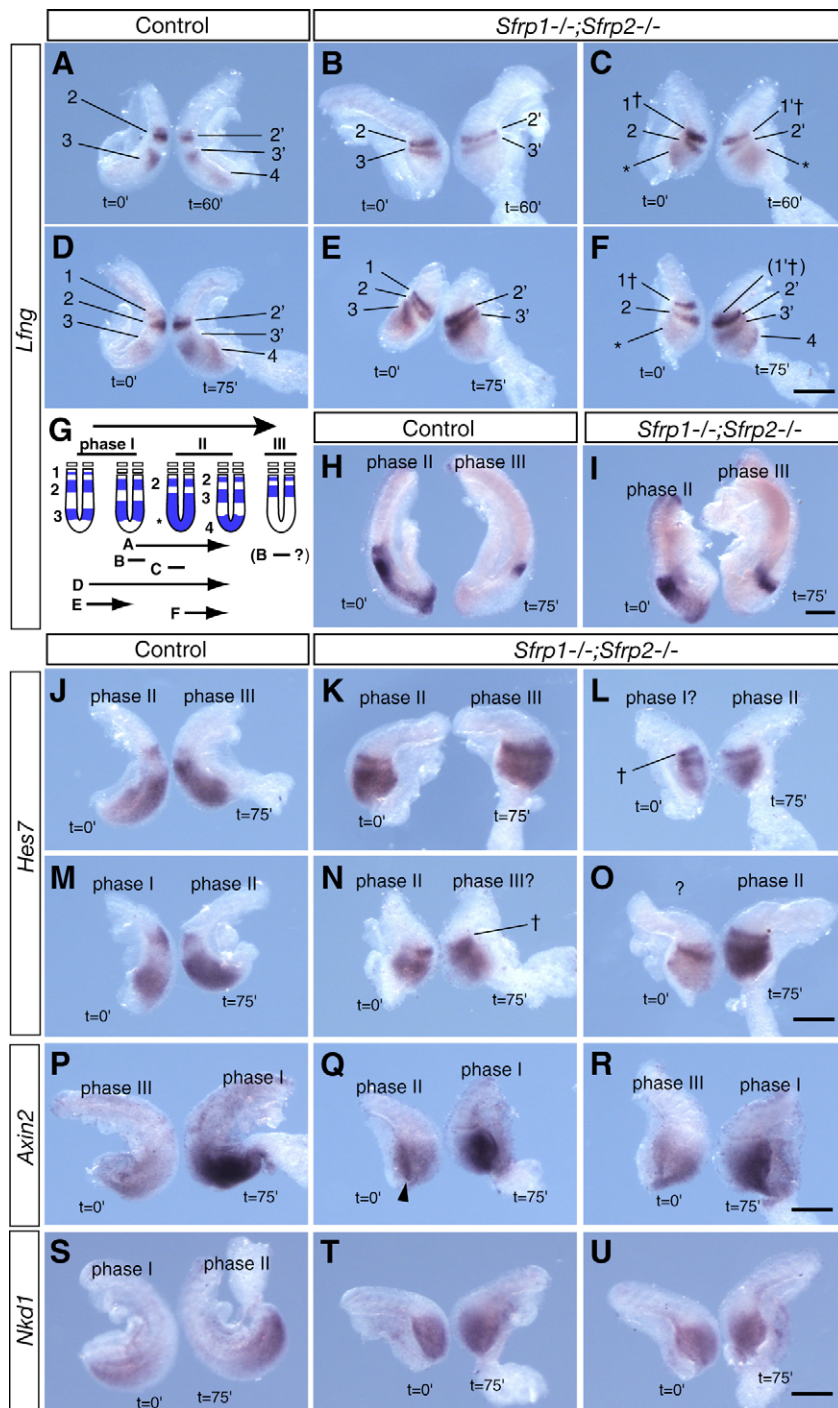
Fig. 7. Perturbed expression of cyclic genes during somitogenesis in *Sfrp1⁻/⁻;Sfrp2⁻/⁻* embryos. (A-G) Altered *Lfng* oscillating cycles in the PSM of *Sfrp1⁻/⁻;Sfrp2⁻/⁻* embryos at E8.5. The *Lfng* cycle was examined in control (A,D) and *Sfrp1⁻/⁻;Sfrp2⁻/⁻* (B,C,E,F) embryos by culture of half of the posterior region for different lengths of time [A, B and C, 0 and 60 minutes (t=0′, 60′); D, E and F, 0 and 75 minutes (t=0′, 75′)]. The dagger indicates a strong extra stripe in the anterior-most region of the PSM. Scale bar: 250 μm. (G) Schematic diagram of *Lfng* expression in control and *Sfrp1⁻/⁻;Sfrp2⁻/⁻* explants. Traveling stripes of *Lfng* expression are indicated by numbers. (H,I) Oscillation pattern of *Lfng* in control (H) and *Sfrp1⁻/⁻;Sfrp2⁻/⁻* (I) explants at E9.5. Half of the posterior region was cultured for either 0 (t=0′) or 75 (t=75′) minutes. Scale bar: 250 μm. (J-U) Expression of *Hes7*, *Axin2* and *Nkx1* in the PSM of *Sfrp1⁻/⁻;Sfrp2⁻/⁻* embryos. Half of the posterior region was cultured for either 0 (t=0′) or 75 (t=75′) minutes. (J-O) *Hes7* expression in control (J,M) and *Sfrp1⁻/⁻;Sfrp2⁻/⁻* (K,L,N,O) explants at E8.5. (L,N,O) *Hes7* expression was perturbed in a large proportion of *Sfrp1⁻/⁻;Sfrp2⁻/⁻* explants. (K) Nearly normal *Hes7* expression cycles were observed in *Sfrp1⁻/⁻;Sfrp2⁻/⁻* explants at lower frequency. The dagger indicates a strong extra stripe in the anterior-most region of the PSM. Scale bar: 250 μm. (P-R) Dynamic expression of *Axin2* in control (P) and *Sfrp1⁻/⁻;Sfrp2⁻/⁻* (Q,R) explants at E8.5. An arrowhead indicates the higher expression domain of *Axin2* in the primitive streak. Stripes of *Axin2* expression were difficult to identify even in control explants at earlier embryonic stages. Scale bar: 250 μm. (S-U) Expression of *Nkd1* in control (S) and *Sfrp1⁻/⁻;Sfrp2⁻/⁻* (T,U) explants at E8.5. Scale bar: 250 μm.

1999b). Although hyperactivation of *T* expression was not detected in the double homozygous mutant embryos, it is possible that moderate levels of activation of expression affect mesoderm cell migration.

Interestingly, the AP axis reduction associated with small somites, and the defect in the craniofacial region and limbs of the *Sfrp1⁻/⁻;Sfrp2⁻/⁻* embryos are similar to the phenotype induced by *Wnt5a* inactivation (Yamaguchi et al., 1999a). Wnt5a is not capable of association with Sfrp1 in vitro (Xu et al., 1998; Dennis et al., 1999), which suggests that Wnt5a signaling is not directly regulated by Sfrp1 and Sfrp2. Previous reports indicated that Wnt5a, which leads to activation of the Wnt/Ca²⁺ pathway, plays a role in canonical Wnt/β-catenin pathway inhibition (Torres et al., 1996; Topol et al.,

2003). Furthermore, the Wnt/Ca²⁺ pathway interacts with the non-canonical PCP pathway (Carreira-Barbosa et al., 2003; Veeman et al., 2003; Westfall et al., 2003). Further analysis is required in order to elucidate the relationship between the roles of Sfrp and Wnt5a. However, these observations suggest that inactivation of *Sfrp1* and *Sfrp2* causes misregulation of a wide spectrum of Wnt activities in the canonical and non-canonical pathways.

Somitogenesis in *Sfrp1⁻/⁻;Sfrp2⁻/⁻* embryos

The segmentation clock in the PSM, which is generated by the expression of oscillator genes, is needed for somite segmentation (Aulehla et al., 2004). A number of oscillator genes, such as *Lfng*,

Her1, chick *hairy1*, chick *hairy2*, *Hes1/Hes2* and *Hes7*, have been identified as components of Notch signaling. In fact, mutations of *Notch*, *Dll1 and Dll3* (Notch ligands), and *Lfng* and *Hes7* (Notch effectors), all result in aberrant segmentation during somitogenesis (Saga and Takeda, 2001; Bessho et al., 2001). The disruption of somite segmentation exhibited by *Sfrp1$^{-/-}$;Sfrp2$^{-/-}$* embryos is associated with altered Notch oscillations, which is supported by abnormal *Lfng* and *Hes7* expression cycles in *Sfrp1$^{-/-}$;Sfrp2$^{-/-}$* embryos.

A Wnt3a gradient in the PSM is thought to function in somitogenesis regulation. Expression of Notch-related oscillator genes is disrupted in *Wnt3a* mutant embryos, which suggests that Wnt acts upstream of Notch signaling (Aulehla et al., 2003). Upregulation of the Wnt/β-catenin pathway was suggested by non-phospho β-catenin staining in the tail bud of *Sfrp1$^{-/-}$;Sfrp2$^{-/-}$* embryos at E8.5. In addition, inactivation of *Sfrp1* and *Sfrp2* perturbed the oscillating expression of *Nkd1*, an oscillator gene activated downstream of Wnt signaling in the PSM (Ishikawa et al., 2004). Moreover, evidence that LEF1/TCF, a downstream mediator of Wnt signaling, activates expression of the Notch ligand *Dll1* revealed the connection between Wnt and Notch signaling (Hofmann et al., 2004; Galceran et al., 2004). These data, and our observations, support the idea that inactivation of *Sfrp1* and *Sfrp2* affects Wnt signaling activity in the PSM in conjunction with the misregulation of oscillating Notch signaling, which results in abnormal of *Lfng* and *Hes7* expression. Interestingly, dynamic expression of *Axin2* in *Sfrp1$^{-/-}$;Sfrp2$^{-/-}$* embryos was observed, suggesting the presence of *Axin2* oscillation. Rapid degradation of the protein may exert an effect on the maintenance of the oscillatory expression cycles even in the PSM of *Sfrp1$^{-/-}$;Sfrp2$^{-/-}$* embryos (Seidensticker and Behrens, 2000; Aulehla et al., 2003). Thus, the intracellular oscillation cycle (*Axin2* expression) does not correlate with the intercellular cycle (*Notch* oscillators) in *Sfrp1$^{-/-}$;Sfrp2$^{-/-}$* embryos, suggesting that Notch signaling is a non-cell autonomous signal that is elevated in Wnt-receiving cells.

In summary, our findings clearly demonstrate the function of *Sfrp1* and *Sfrp2* in AP axis elongation and somitogenesisis. Because Sfrps regulate a wide spectrum of Wnt activities and pathways, these results suggest that coordinated regulation in the canonical and non-canonical Wnt pathways plays a significant role in embryonic patterning.

Supplementary material
Supplementary material for this article is available at
http://dev.biologists.org/cgi/content/full/133/6/989/DC1

References
Agathon, A., Thisse, C. and Thisse, B. (2003). The molecular nature of the zebrafish tail organizer. *Nature* **424**, 448-452.
Aulehla, A. and Herrmann, B., G. (2004). Segmentation in vertebrates: clock and gradient finally joined. *Genes Dev.* **18**, 2060-2067.
Aulehla, A., Wehrle, C., Brand-Saberi, B., Kemler, R., Gossler, A., Kanzler, B. and Herrmann, B. G. (2003). *Wnt3a* plays a major role in the segmentation clock controlling somitogenesis. *Dev. Cell* **4**, 395-406.

Barrow, J. R., Thomas, K. R., Boussadia-Zahui, O., Moore, R., Kemler, R., Capecchi, M. R. and McMahon, A. P. (2003). Ectodermal *Wnt3*/b-catenin signaling is required for the establishment and maintenance of the apical ectodermal ridge. *Genes Dev.* **17**, 394-409.
Bessho, Y., Sakata, R., Komatsu, S., Shiota, K., Yamada, S. and Kageyama, R. (2001). Dynamic expression and essential functions of *Hes7* in somite segmentation. *Genes Dev.* **15**, 2642-2647.
Bessho, Y., Hirata, H., Masamizu, Y. and Kageyama, R. (2003). Periodic repression by the bHLH factor Hes7 is an essential mechanism for the somite segmentation clock. *Genes Dev.* **17**, 1451-1456.
Bettenhausen, B., Hrabe de Angelis, M., Simon, D., Guenet, J. L. and Gossler, A. (1995). Transient and restricted expression during mouse embryogenesis of *Dll1*, a murine gene closely related to *Drosophila* Delta. *Development* **121**, 2407-2418.
Bodine, P. V., Zhao, W., Kharode, Y. P., Bex, F. J., Lambert, A. J., Goad, M. B., Gaur, T., Stein, G. S., Lian, J. B. and Komm, B. S. (2004). The Wnt antagonist secreted frizzled-related protein-1 is a negative regulator of trabecular bone formation in adult mice. *Mol. Endocrinol.* **18**, 1222-1237.
Candia, A. F., Hu, J., Crosby, J., Lalley, P. A., Noden, D., Nadeau, J. H. and Wright, C. V. (1992). *Mox-1* and *Mox-2* define a novel homeobox gene subfamily and are differentially expressed during early mesodermal patterning in mouse embryos. *Development* **116**, 1123-1136.
Carreira-Barbosa, F., Concha, M. L., Takeuchi, M., Ueno, N., Wilson, S. W. and Tada, M. (2003). Prickle 1 regulates cell movements during gastrulation and neuronal migration in zebrafish. *Development* **130**, 4037-4046.
Chadee, D. N., Taylor, W. R., Hurta, R. A., Allis, C. D., Wright, J. A. and Davie, J. R. (1995). Increased phosphorylation of histone H1 in mouse fibroblasts transformed with oncogenes or constitutively active mitogen-activated protein kinase. *J. Biol. Chem.* **270**, 20098-20105.
Chapman, D. L., Agulnik, I., Hancock, S., Silver, L. M. and Papaioannou, V. E. (1996). Tbx6, a mouse T-Box gene implicated in paraxial mesoderm formation at gastrulation. *Dev. Biol.* **180**, 534-542.
Cole, S. E., Levorse, J. M., Tilghman, S. M. and Vogt, T. F. (2002). Clock regulatory elements control cyclic expression of *Lunatic fringe* during somitogenesis. *Dev. Cell* **3**, 75-84.
Correia, K. M. and Conlon. R. A. (2000). Surface ectoderm is necessary for the morphogenesis of somites. *Mech. Dev.* **91**, 19-30.
Corson, L. B., Yamanaka, Y., Lai, K. M. and Rossant, J. (2003). Spatial and temporal patterns of ERK signaling during mouse embryogenesis. *Development* **130**, 4527-4537.
Dennis, S., Aikawa, M., Szeto, W., d'Amore, P. A. and Papkoff, J. (1999). A secreted frizzled related protein, FrzA, selectively associates with Wnt-1 protein and regulates wnt-1 signaling. *J. Cell Sci.* **112**, 3815-3820.
Dodd, J., Morton, S. B., Karagogeos, D., Yamamoto, M. and Jessell, T. M. (1988). Spatial regulation of axonal glycoprotein expression on subsets of embryonic spinal neurons. *Neuron* **1**, 105-116.
Edmondson, D. G. and Olson, E. N. (1989). A gene with homology to the myc similarity region of MyoD1 is expressed during myogenesis and is sufficient to activate the muscle differentiation program. *Genes Dev.* **3**, 628-640.
Evrard, Y. A., Lun, Y., Aulehla, A., Gan, L. and Johnson, R. L. (1998). *Lunatic fringe* is an essential mediator of somite segmentation and patterning. *Nature* **394**, 377-381.
Finley, K. R., Tennessen, J. and Shawlot, W. (2003). The mouse *secreted frizzled-related protein* 5 gene is expressed in the anterior visceral endoderm and foregut endoderm during early post-implantation development. *Gene Expr. Patterns* **3**, 681-684.
Forsberg, H., Crozet, F. and Brown, N. A. (1998). Waves of mouse *Lunatic fringe* expression, in four-hour cycles at two-hour intervals, precede somite boundary formation. *Curr. Biol.* **8**, 1027-1030.
Galceran, J., Sustmann, C., Hsu, S. C., Folberth, S. and Grosschedl, R. (2004). LEF1-mediated regulation of *Delta-like1* links Wnt and Notch signaling in somitogenesis. *Genes Dev.* **18**, 2718-2723.
Glinka, A., Wu, W., Onichtchouk, D., Blumenstock, C. and Niehrs, C. (1997). Head induction by simultaneous repression of Bmp and Wnt signaling in *Xenopus*. *Nature* **389**, 517-519.
Goulding, M. D., Chalepakis, G., Deutsch, U., Erselius, J. R. and Gruss, P. (1991). *Pax-3*, a novel murine DNA binding protein expressed during early neurogenesis. *EMBO J.* **10**, 1135-1147.
Guo, X., Day, T. F., Jiang, X., Garrett-Beal, L., Topol, L. and Yang, Y. (2004). Wnt/beta-catenin signaling is sufficient and necessary for synovial joint formation. *Genes Dev.* **18**, 2404-2417.
Heisenberg, C. P., Tada, M., Rauch, G. J., Saude, L., Concha, M. L., Geisler, R., Stemple, D. L., Smith, J. C. and Wilson, S. W. (2000). Silberblick/Wnt11 mediates convergent extension movements during zebrafish gastrulation. *Nature* **405**, 76-81.
Hérault, Y., Beckers, J., Kondo, T., Fraudeau, N. and Duboule, D. (1998). Genetic analysis of a *Hoxd-12* regulatory element reveals global versus local modes of controls in the *HoxD* complex. *Development* **125**, 1669-1677.
Hofmann, M., Schuster-Gossler, K., Watabe-Rudolph, M., Aulehla, A., Herrmann, B. G. and Gossler, A. (2004). WNT signaling, in synergy with

T/TBX6, controls Notch signaling by regulating *Dll1* expression in the presomitic mesoderm of mouse embryos. *Genes Dev*. **18**, 2712-2717.

Houart, C., Caneparo, L., Heisenberg, C., Barth, K., Take-Uchi, M. and Wilson, S. (2002). Establishment of the telencephalon during gastrulation by local antagonism of Wnt signaling. *Neuron* **35**, 255-265.

Hsieh, J. C., Kodjabachian, L., Rebbert, M. L., Rattner, A., Smallwood, P. M., Samos, C. H., Nusse, R., Dawid, I. B. and Nathans, J. (1999). A new secreted protein that binds to Wnt proteins and inhibits their activities. *Nature* **398**, 431-436.

Ishikawa, A., Kitajima, S., Takahashi, Y., Kokubo, H., Kanno, J., Inoue, T. and Saga, Y. (2004). Mouse Nkd1, a Wnt antagonist, exhibits oscillatory gene expression in the PSM under the control of Notch signaling. *Mech. Dev*. **121**, 1443-1453.

Itasaki, N., Jones, C. M., Mercurio, S., Rowe, A., Domingos, P. M., Smith, J. C. and Krumlauf, R. (2003). Wise, a context-dependent activator and inhibitor of Wnt signaling. *Development* **130**, 4295-4305.

Jones, S. E. and Jomary, C. (2002). Secreted Frizzled-related proteins: searching for relationships and patterns. *Bioessays* **24**, 811-820.

Kawano, Y. and Kypta, R. (2003). Secreted antagonists of the Wnt signaling pathway. *J. Cell Sci*. **116**, 2627-2634.

Kelly, O. G., Pinson, K. I. and Skarnes, W. C. (2004). The Wnt co-receptors Lrp5 and Lrp6 are essential for gastrulation in mice. *Development* **131**, 2803-2815.

Kühl, M. (2002). Non-canonical Wnt signaling in *Xenopus*: regulation of axis formation and gastrulation. *Semin. Cell Dev. Biol*. **13**, 243-249.

Lee, C. S., Buttitta, L. A., May, N. R., Kispert, A. and Fan, C. M. (2000). SHH-N upregulates *Sfrp2* to mediate its competitive interaction with WNT1 and WNT4 in the somitic mesoderm. *Development* **127**, 109-118.

Leimeister, C., Bach, A. and Gessler, M. (1998). Developmental expression patterns of mouse sFRP genes encoding members of the secreted frizzled related protein family. *Mech. Dev*. **75**, 29-42.

Leyns, L., Bouwmeester, T., Kim, S. H., Piccolo, S and De Robertis, E. M. (1997). Frzb-1 is a secreted antagonist of Wnt signaling expressed in the Spemann organizer. *Cell* **88**, 747-756.

Li, Z. L. and Shiota, K. (1999). Stage-specific homeotic vertebral transformations in mouse fetuses induced by maternal hyperthermia during somitogenesis. *Dev. Dyn*. **216**, 336-348.

Liu, P, Wakamiya, M., Shea, M. J., Albrecht, U., Behringer, R. R. and Bradley, A. (1999). Requirement for *Wnt3* in vertebrate axis formation. *Nat. Genet*. **22**, 361-365.

Mansouri, A., Yokota, Y., Wehr, R., Copeland, N. G., Jenkins, N. A. and Gruss, P. (1997). Paired-related murine homeobox gene expressed in the developing sclerotome, kidney, and nervous system. *Dev. Dyn*. **210**, 53-65.

Maruoka, Y., Ohbayashi, N., Hoshikawa, M., Itoh, N., Hogan, B. L. and Furuta, Y. (1998). Comparison of the expression of three highly related genes, *Fgf8, Fgf17* and *Fgf18*, in the mouse embryo. *Mech. Dev*. **74**, 175-177.

Melkonyan, H. S., Chang, W. C., Shapiro, J. P, Mahadevappa, M., Fitzpatrick, P. A., Kiefer, M. C., Tomei, L. D. and Umansky, S. R. (1997). SARPs: a family of secreted apoptosis-related proteins. *Proc. Natl. Acad. Sci. USA* **94**, 13636-13641.

Morales, A. V., Yasuda, Y. and Ish-Horowicz, D. (2002). Periodic *Lunatic fringe* expression is controlled during segmentation by a cyclic transcriptional enhancer responsive to notch signaling. *Dev. Cell* **3**, 63-74.

Mukhopadhyay, M., Shtrom, S., Rodriguez-Esteban, C., Chen, L., Tsukui, T., Gomer, L., Dorward, D. W., Glinka, A., Grinberg, A., Huang, S. P. et al. (2001). *Dickkopf1* is required for embryonic head induction and limb morphogenesis in the mouse. *Dev. Cell*. **1**, 423-434.

Mukhopadhyay, M., Teufel, A., Yamashita, T., Agulnick, A. D., Chen, L., Downs, K. M., Schindler, A., Grinberg, A., Huang, S. P., Dorward, D. et al. (2003). Functional ablation of the mouse *Ldb1* gene results in severe patterning defects during gastrulation. *Development* **130**, 495-505.

Neubuser, A., Koseki, H. and Balling, R. (1995). Characterization and developmental expression of *Pax9*, a paired-box-containing gene related to *Pax1*. *Dev. Biol*. **170**, 701-716.

Niehrs, C. (1999). Head in the WNT: the molecular nature of Spemann's head organizer. *Trends Genet*. **15**, 314-319.

Perea-Gomez, A., Vella, F. D., Shawlot, W., Oulad-Abdelghani, M., Chazaud, C., Meno, C., Pfister, V., Chen, L., Robertson, E., Hamada, H. et al. (2002). Nodal antagonists in the anterior visceral endoderm prevent the formation of multiple primitive streaks. *Dev. Cell* **3**, 745-756.

Rossel, M. and Capecchi, M. R. (1999). Mice mutant for both *Hoxa1* and *Hoxb1* show extensive remodeling of the hindbrain and defects in craniofacial development. *Development* **126**, 5027-5040.

Rosso, S. B., Sussman, D., Wynshaw-Boris, A. and Salinas, P. C. (2005). Wnt signaling through Dishevelled, Rac and JNK regulates dendritic development. *Nat. Neurosci*. **8**, 34-42.

Saga, Y. and Takeda, H. (2001). The making of the somite: molecular events in vertebrate segmentation. *Nat. Rev. Genet*. **2**, 835-845.

Seidensticker, M. J. and Behrens, J. (2000). Biochemical interactions in the wnt pathway. *Biochim. Biophys. Acta*. **1495**, 168-1682.

Semënov, M. V., Tamai, K., Brott, B. K., Kuhl, M., Sokol, S. and He, X. (2001). Head inducer Dickkopf-1 is a ligand for Wnt coreceptor LRP6. *Curr. Biol*. **26**, 951-961.

Shawlot, W. and Behringer, R. R. (1995). Requirement for *Lim1* in head-organizer function. *Nature* **374**, 425-430.

Shawlot, W., Wakamiya, M., Kwan, K. M., Kania, A., Jessell, T. M. and Behringer, R. R. (1999). *Lim1* is required in both primitive streak-derived tissues and visceral endoderm for head formation in the mouse. *Development* **126**, 4925-4932.

Shimono, A. and Behringer, R. R. (1999). Isolation of novel cDNAs by subtractions between the anterior mesendoderm of single mouse gastrula stage embryos. *Dev. Biol*. **209**, 369-380.

Shimono, A. and Behringer, R. R. (2000). Differential screens with subtracted PCR-generated cDNA libraries from subregions of single mouse embryos. *Methods Mol. Biol*. **136**, 333-344.

Shimono, A. and Behringer, R. R. (2003). Angiomotin regulates visceral endoderm movements during mouse embryogenesis. *Curr. Biol*. **13**, 613-617.

Soshnikova, N., Zechner, D., Huelsken, J., Mishina, Y., Behringer, R. R., Taketo, M. M., Crenshaw, E. B., 3rd and Birchmeier, W. (2003). Genetic interaction between Wnt/b-catenin and BMP receptor signaling during formation of the AER and the dorsal-ventral axis in the limb. *Genes Dev*. **17**, 1963-1968.

Suzuki, H., Watkins, D. N., Jair, K. W., Schuebel, K. E., Markowitz, S. D., Dong Chen, W., Pretlow, T. P., Yang, B., Akiyama, Y., Van Engeland, M. et al. (2004). Epigenetic inactivation of *SFRP* genes allows constitutive WNT signaling in colorectal cancer. *Nat. Genet*. **36**, 417-422.

Takada, S., Stark, K. L., Shea, M. J., Vassileva, G., McMahon, J. A. and McMahon, A. P. (1994). *Wnt-3a* regulates somite and tailbud formation in the mouse embryo. *Genes Dev*. **8**, 174-189.

Topol, L., Jiang, X., Choi, H., Garrett-Beal, L., Carolan, P. J. and Yang, Y. (2003). Wnt-5a inhibits the canonical Wnt pathway by promoting GSK-3-independent beta-catenin degradation. *J. Cell Biol*. **162**, 899-908.

Torres, M. A., Yang-Snyder, J. A., Purcell, S. M., DeMarais, A. A., McGrew, L. L. and Moon, R. T. (1996). Activities of the *Wnt-1* class of secreted signaling factors are antagonized by the *Wnt-5A* class and by a dominant negative cadherin in early *Xenopus* development. *J. Cell Biol*. **133**, 1123-1137.

Ulrich, F., Concha, M. L., Heid, P. J., Voss, E., Witzel, S., Roehl, H., Tada, M., Wilson, S. W., Adams, R. J., Soll, D. R. et al. (2003). Slb/Wnt11 controls hypoblast cell migration and morphogenesis at the onset of zebrafish gastrulation. *Development* **130**, 5375-5384.

Veeman, M. T., Slusarski, D. C., Kaykas, A., Louie, S. H. and Moon, R. T. (2003). Zebrafish prickle, a modulator of noncanonical Wnt/Fz signaling, regulates gastrulation movements. *Curr. Biol*. **13**, 680-685.

Wakamatsu, Y., Watanabe, Y., Shimono, A. and Kondoh, H. (1993). Transition of localization of the N-Myc protein from nucleus to cytoplasm in differentiating neurons. *Neuron* **10**, 1-9.

Wang, S., Krinks, M., Lin, K., Luyten, F. P. and Moos, M., Jr (1997). Frzb, a secreted protein expressed in the Spemann organizer, binds and inhibits Wnt-8. *Cell* **88**, 757-766.

Westfall, T. A., Brimeyer, R., Twedt, J., Gladon, J., Olberding, A., Furutani-Seiki, M. and Slusarski, D. C. (2003). Wnt-5/pipetail functions in vertebrate axis formation as a negative regulator of Wnt/beta-catenin activity. *J. Cell Biol*. **162**, 889-898.

Wilkinson, D. G. (ed.) (1992). *In Situ Hybridization*, pp. 75-83. Oxford: IRL.

Wilkinson, D. G., Bhatt, S. and Herrmann, B. G. (1990). Expression pattern of the mouse T gene and its role in mesoderm formation. *Nature* **343**, 657-659.

Wilson, V., Rashbass, P. and Beddington, R. S. (1993). Chimeric analysis of T (*Brachyury*) gene function. *Development* **117**, 1321-1331.

Xu, Q., D'Amore, P. A. and Sokol, S. Y. (1998). Functional and biochemical interactions of Wnts with FrzA, a secreted Wnt antagonist. *Development* **125**, 4767-4776.

Yamaguchi, T. P. (2001). Heads or tails: Wnts and anterior-posterior patterning. *Curr. Biol*. **11**, R713-R724.

Yamaguchi, T. P., Bradley, A., McMahon, A. P. and Jones, S. (1999a). A *Wnt5a* pathway underlies outgrowth of multiple structures in the vertebrate embryo. *Development* **126**, 1211-1223.

Yamaguchi, T. P., Takada, S., Yoshikawa, Y., Wu, N. and McMahon, A. P. (1999b). T (*Brachyury*) is a direct target of Wnt3a during paraxial mesoderm specification. *Genes Dev*. **13**, 3185-3190.

Yan, D., Wallingford, J. B., Sun, T. Q., Nelson, A. M., Sakanaka, C., Reinhard, C., Harland, R. M., Fantl, W. J. and Williams, L. T. (2001). Cell autonomous regulation of multiple Dishevelled-dependent pathways by mammalian Nkd. *Proc. Natl. Acad. Sci. USA* **98**, 3802-3807.

Yoshikawa, Y., Fujimori, T., McMahon, A. P. and Takada, S. (1997). Evidence that absence of Wnt-3a signaling promotes neuralization instead of paraxial mesoderm development in the mouse. *Dev. Biol*. **183**, 234-242.

Yoshino, K., Rubin, J. S., Higinbotham, K. G., Uren, A., Anest, V., Plisov, S. Y. and Perantoni, A. O. (2001). Secreted Frizzled-related proteins can regulate metanephric development. *Mech. Dev*. **102**, 45-55.